P.147 MICROPHYSICAL PROPERTIES OF SUBVISIBLE CIRRUS

R. Paul Lawson*, Bryan Pilson, Brad Baker and Qixu Mo
SPEC Incorporated, Boulder Colorado

1. INTRODUCTION

Subvisible cirrus (SVC) clouds appear mostly below the tropopause, especially in the tropics (Beyerle et al. 1998; McFarquhar et al. 2000) and at midlatitudes (Sassen and Campbell 2001). They are occasionally observed above the tropopause at midlatitudes (Goldfarb et al. 2001) and in polar regions (Lelieveld et al., 1999; K¨archer and Solomon, 1999). Supersaturation with respect to ice, sometimes exceeding 100%, has been observed in the upper troposphere and lowermost stratosphere (Murphy et al. 1990; Gierens et al. 1999; Ovarlez et al. 2000; Jensen et al. 2001). A visible optical depth of τ = 0.03 for SVC was established as a threshold by Sassen et al. (1989) using lidar and radiation flux measurements. I has been suggested that SVC can effectively freeze-dry air crossing the tropical tropopause to the observed lower stratospheric water vapor concentrations (Jensen et al. 1996), and may significantly affect the Earth's radiation budget (Comstock et al. 2002).

Figure 1. Photograph of (top) subvisible cirrus observed by (bottom) the NASA WB-57F during transit flight from Houston, Texas for the Costa Rica - Aura Validation Experiment (CR-AVE).

*Corresponding Author Address: Dr. R. Paul Lawson
SPEC Inc. 3022 Sterling Circle, Boulder, CO 80301
Email: plawson@specinc.com

Subvisible cirrus clouds were studied with the NASA WB-57F research aircraft in January - February 2006 during the Costa Rica – Aura Validation Experiment (CR-AVE http://cloud1.arc.nasa.gov/ave-costarica2). While there have been several studies of SVC using airborne, satellite and ground-based lidar, there has been a relative dearth of in situ microphysical measurements.

2. INSTRUMENTATION

A highlight of CR-AVE was the full complement of state-of-the art microphysical probes used to extensively investigate SVC. The WB-57F was equipped with a suite of 29 sensors. Instruments discussed in this paper include a cloud particle imager (CPI) (Lawson et al. 2001), a cloud and aerosol particle spectrometer (CAPS) (Baumgardner et al. 2001), a tunable diode laser hygrometer (May 1998) and a 2D-S (stereo) optical imaging probe (Lawson et al. 2006). The SPEC CPI and 2D-S probes are shown in **Fig. 2**.

The combination of particle probes provided extensive overlap in particle size distributions and high-resolution digital images of the particles in SVC. The CAPS contains two particle probes, a cloud and aerosol spectrometer (CAS), which measures forward and backward light-scattering of particles from 1 to 50 μm, and a cloud imaging probe (CIP) that images particles from 50 to 1600 μm. The CPI provides very good digital images of ice particles in SVC, but its small sample volume compared with the optical array probes limits its ability to adequately represent the entire particle size distribution. The 2D-S is a new imaging probe that has true 10 μm pixel resolution, whereas the response of the older 2D imaging probes is degraded with airspeed. At the true airspeed of the WB-57F (about 170 m s^{-1} at 55,000 ft), the older 2D imaging probes do not detect particles with sizes less than 50 to 100 μm (Lawson et al. 2006).

The ability of the 2D-S to reliably image particles from about 10 to 1200 μm facilitates re-sizing out-of-focus images, a source of error that has hampered older 2D imaging probes (Korolev et al. 1998). Examples of 2D-S images in SVC and a re-sized image using an algorithm developed by Korolev (2006 – personal communication) are shown in **Fig. 3**. The algorithm is based on theoretical diffraction and has been evaluated using images of glass beads in the laboratory. **Figure 4** shows an example of re-sizing 100 μm out-of-focus glass beads using the Korolev algorithm. The Korolev algorithm was tested on several bead sizes, and it performed better on some sizes than it did on others, for reasons that are unknown at this time. **Figure 4** is one of the better cases, with other bead sizes performing worse and a few performing better.

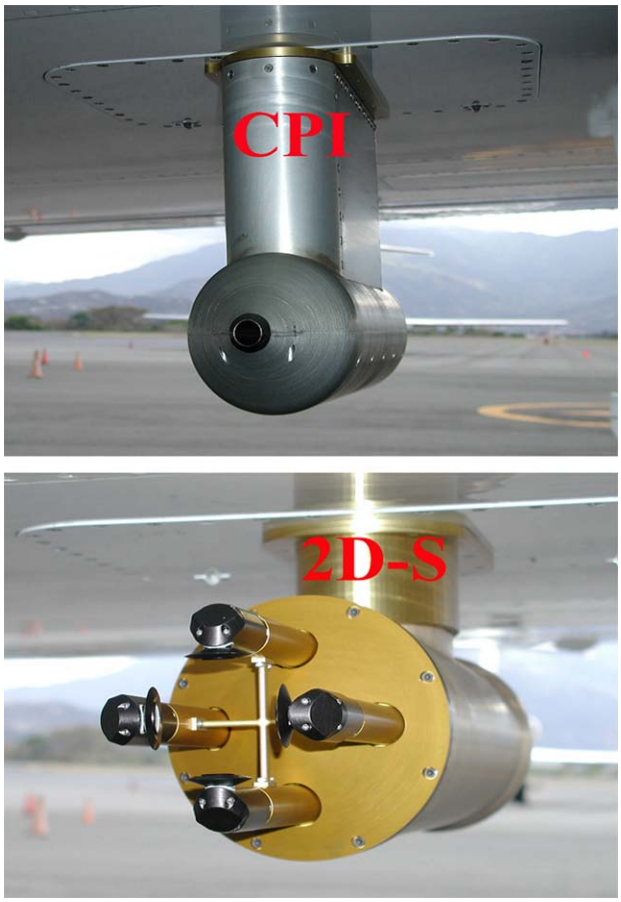

Figure 2. Photographs of the CPI and 2D-S probes installed under the right wing of the NASA WB-57F for the CR-AVE project.

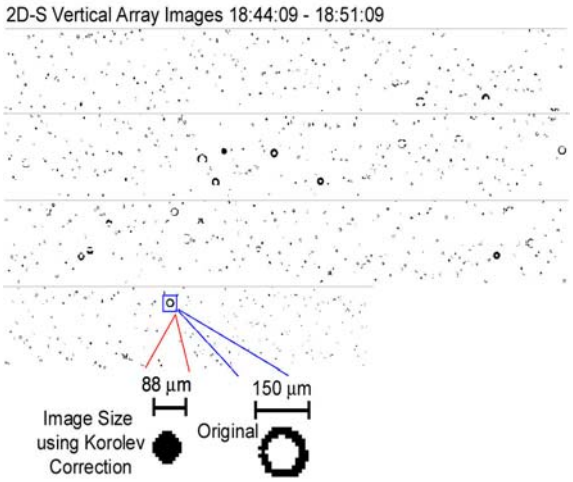

Figure 3. 2D-S particle images from the vertical (V) channel of the 2D-S probe and an example of size correction of an out-of-focus image using the Korolev resizing scheme.

3. DATA

Figure 5 shows the WB-57F flight track on the transit flight to San Jose, Costa Rica and tracks for five research flights (RF 1, 5, 8, 9 and 11). Also shown in **Fig. 5** are vertical profiles of the transit flight and research flights where SVC was observed by the WB-57F. The data in **Fig. 5** show that SVC was frequently observed and that it was consistently found between about 53,000 and 58,000 ft msl, which corresponds to a temperature range from about – 75 to – 85°C.

The vertical location and microphysical properties of the SVC observed during CR-AVE are very consistent. **Figure 6** shows an example of SVC particle size distributions observed by the CPI and 2D-S probes, along with a composite size distribution using the CAS and 2D-S and examples of CPI images. Also shown in **Figure 6**, for the sake of comparison, are particle size distributions and CPI images when the WB-57F flew through its own contrail during an SVC mission. **Figure 7** shows a histogram of particle habits from all of the CR-AVE missions where SVC was encountered. The particles habits were determined by visual classification by a trained analyst. As seen in **Figs. 6** and **7**, the large majority (84%)of the particles in SVC are spherical in shape and < 100 µm in maximum dimension.

On very rare occasions, some larger particles (with sizes up to about 120 µm) were imaged by the 2D-S probe, but their numbers were not sufficient to be statistically significant. The larger

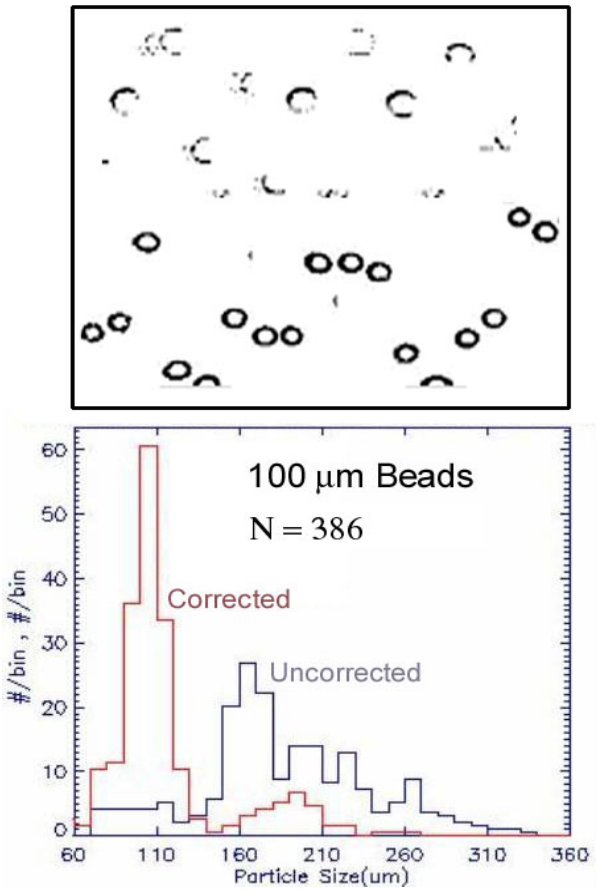

Figure 4. Examples of (top) 2D-S out-of-focus images of 100 µm glass beads and (bottom) uncorrected and corrected size distributions using the Korolev algorithm.

particles were generally plate or columnar in shape.

The data in **Figs. 6** and **7** are in contrast to the only other (Heymsfield (1986) observation of particle shapes, which were made in a high altitude cirrus cloud made by the WB-57F over the Marshall Islands. Heymsfield examined replicator data collected on 17 December 1973 in a thin cirrus cloud within a temperature range from –83 to –84°C. The particle sizes ranged from about 5 to 50 µm and particle shapes consisted of about 50% trigonal plates and 50% columns. The CR-AVE data suggests that the SVC observed near Costa Rica consisted of slightly larger particles with a considerably different mixture of crystal habits. Only 4 trigonal plates (0.06%, 177 columns (2.91%) and 149 hexagonal plates (2.46%) were observed out of a total of 6071 particles analyzed in the CR-AVE SVC data set.

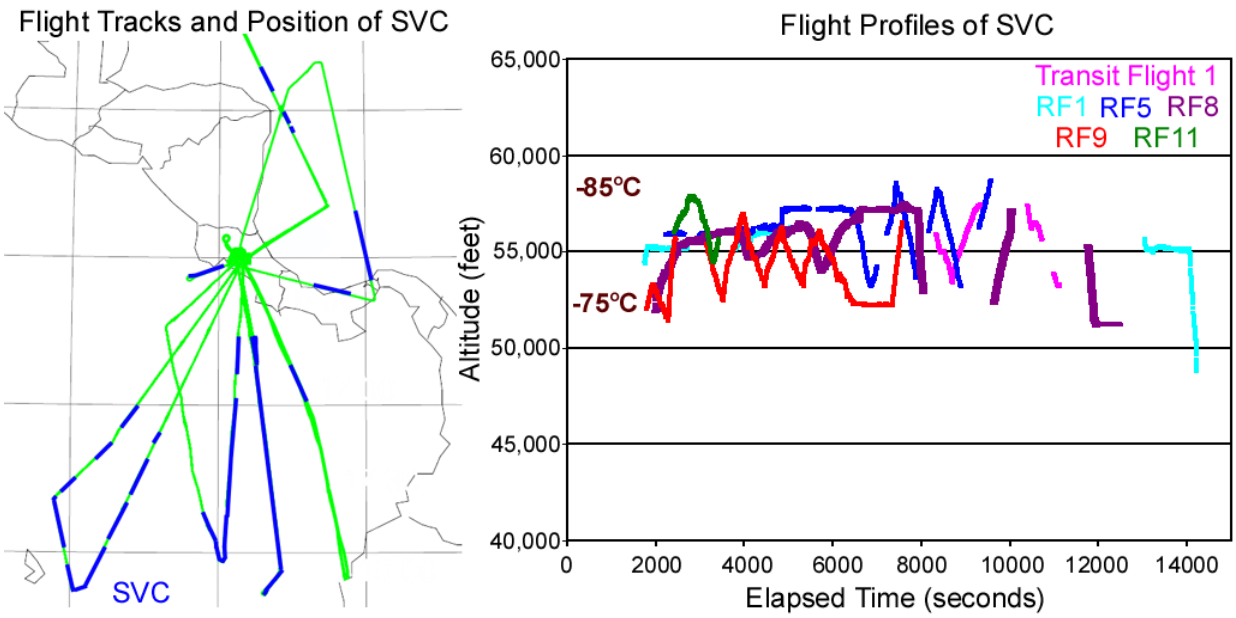

Figure 5. (left) WB-57F flight tracks during CR-AVE showing (in blue) regions where SVC was encountered and (right) vertical profile showing location of SVC. The color code in the right panel corresponds with the research flight (RF) number shown in the legend

The lack of trigonal ice in the SVC data set is curious. The replicator images shown in Heymsfield (1986) are clearly trigonal. The CPI images are not quite as sharp as the replicator images, but once particles are larger than about 25 μm, trigonal shapes would be clearly identifiable if they existed. This has been verified using a reticule in the laboratory. Thus, the differences in particle habits between the Heymsfield (1986) case and the CR-AVE data set cannot be attributed to instrumental effects. The data set collected in 1973 is 32 years previous to the CR-AVE data, and the possibility exists that differences in the aerosol and moisture fields have changed over the past three decades; however, this possibility cannot be tested, since reliable aerosol and moisture measurements were not made in 1973.

The size range of particles in the CR-AVE data set appear to extend to larger sizes than previously observed in SVC. For example, the average particle size distribution in **Fig. 6** extends out to 100 μm, and on rare occasions particles as large as 120 μm have been observed. McFarquhar et al. (2000) extended analysis of the Heymsfield (1986) data, which, along with the replicator previously mentioned, was collected using a Particle Measuring Systems (PMS) axially scattering probe and a PMS 1D cloud probe. The bulk properties (i.e., number concentration, extinction, ice water content, visible optical depth) reported by McFarquhar et al. (2000) in SVC are generally similar to those observed during CR-AVE and shown in **Fig. 6**. However, Heymsfield (1986) and McFarquhar et al. (2000) both report that the particle sizes did not extend past 50 μm. McFarquhar et al. do mention that collateral studies with the Aeromet Learjet near the Marshall Islands using PMS probes recorded ice particles up to 140 μm in SVC between 14 and 15 km (45,000 and 49,000 ft).

While the larger particles occasionally observed during CR-AVE do not have a significant impact on bulk microphysical properties, they do raise the question of how such relatively large particles can exist at these high altitudes. The large-scale vertical velocities at (16.7 to 18.3 km) 55,000 to 60,000 ft in the tropics are expected to be low, on the order of a few cm s^{-1}, while the fall velocity of 100 μm C1g ice particles is on the order of 25 cm s^{-1} at this altitude (Jensen et al. 2006). This suggests that these larger particles should fall out of the SVC in about 1 h, which is barely enough time to grow to 100 μm, unless the ice supersaturations are on the order of 100% (Jensen et al. 2006).

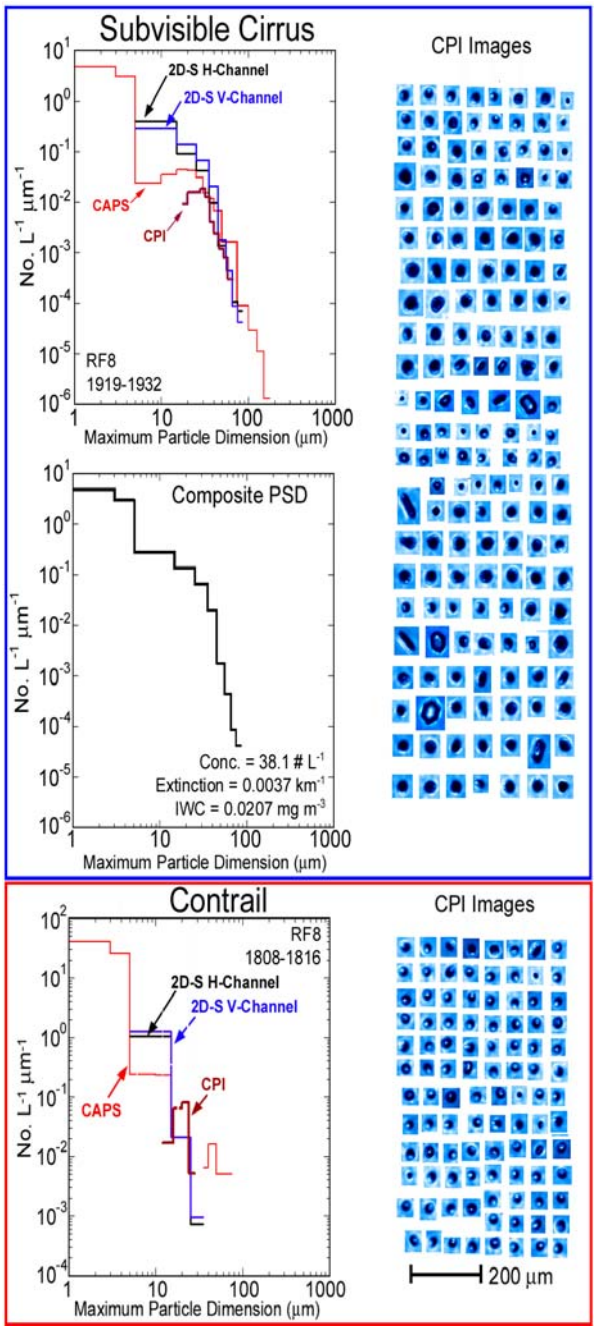

Figure 6. Example of (top and middle) SVC particle size distributions from CAPS, CPI and 2D-S probes and CPI images and a composite size distribution made from the CAS and 2D-S

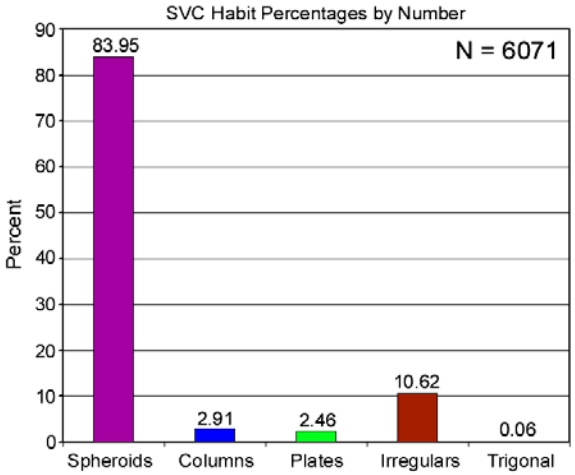

Figure 7. Histogram of particle habits in SVC based on 6071 images classified by eye.

The concentration of water vapor near the tropical tropopause has been measured using several techniques. A more detailed discussion of these measurements is given in Jensen et al. (2006) and is beyond the scope of this paper. However, suffice it to say that there are wide discrepancies between measurements. The discrepancies include relatively small differences between measurements on the WB-57F and larger disagreements with balloon-borne measurements, which show much lower relative humidity near the tropical tropopause. **Figure 8** shows time-series measurements in SVC using the Jet Propulsion Laboratory (JPL) TDL relative humidity and CPI data. Since the CAS and 2D-S data are not included in this figure, the small and large ends of the particle size distribution are not represented. Thus, the number concentration is underestimated, but the extinction and ice water content values are mostly accurate, since the CPI captures the majority of area and mass measurements within its size range.

The data in **Fig. 8** show that SVC is generally encountered within a range of RH_{ice} from about 140 to 160%. Jensen et al. (2006) report that, compared with a Harvard Lyman-α device, the JPL RH_{ice} value may even be too low, suggesting that the actual RH_{ice} may be closer to 200%. Jensen et al. (2006) base their suggestion on an ice particle growth model, which predicts that values of about 200% are necessary to account for observations of 50 to 100 µm ice within 500 m of the tropopause.

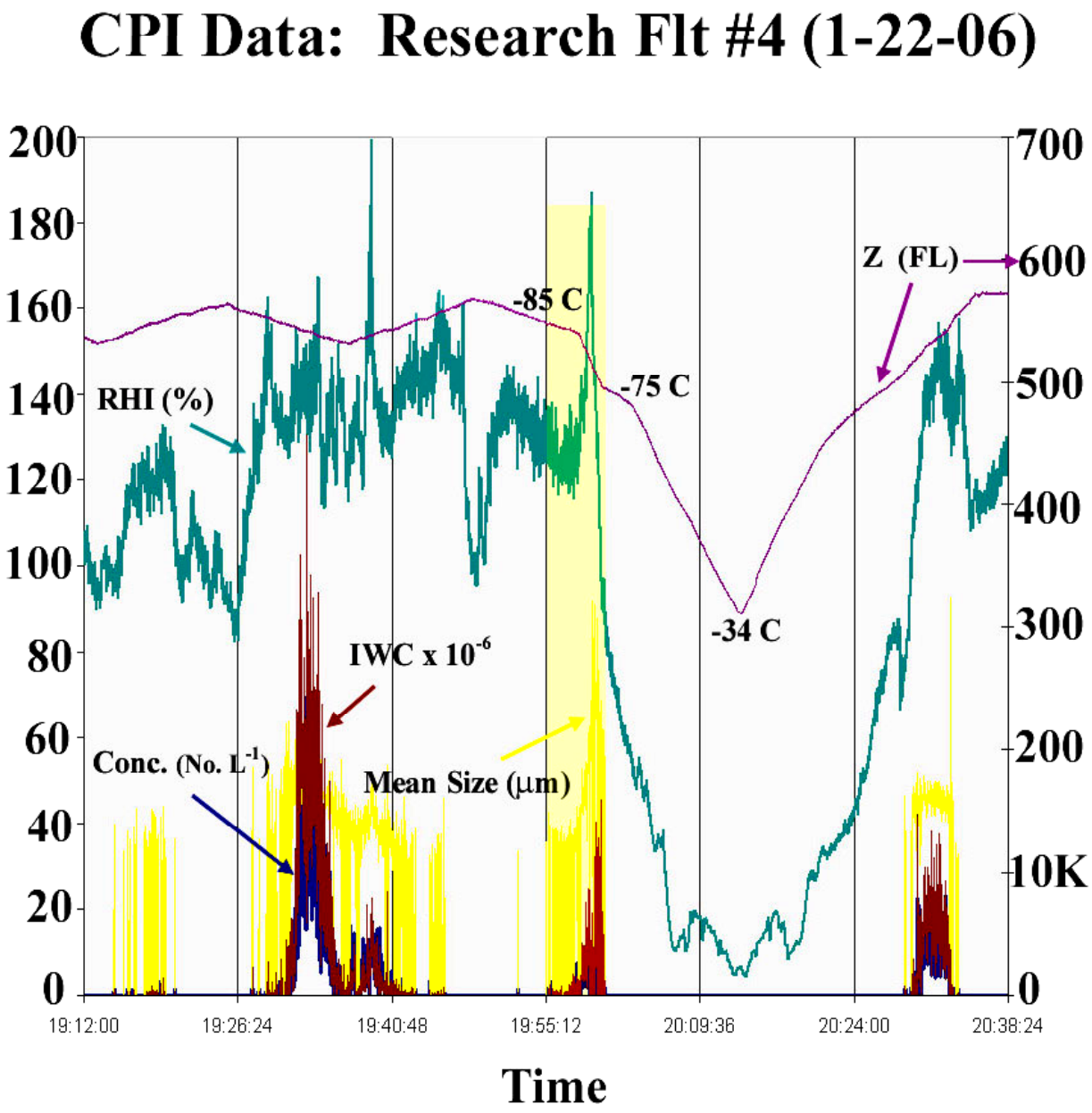

Figure 8. Example of time series measurements showing JPL relative humidity (RHI in green) and measurements from the CPI in SVC. All values are referenced to the left vertical scale except altitude (Z ft), which is referenced to the right vertical scale.

4. SUMMARY

During the 2006 CR-AVE project staged from Costa Rica, the NASA WB-57F often observed SVC within about 1 km of the tropopause between about 0 and 10° N Latitude. The average ice particle number concentration (38 L^{-1}), extinction coefficient (0.0037 km^{-1}), ice water content (0.02 mg m^{-3}) and optical depth (0.006) are similar to values computed from in situ measurements over the Marshall Islands by McFarquhar et al. (2000). However, CPI images of the ice particles observed in CR-AVE were markedly different, with 84% of the particles being quasi-spherical, while McFarquhar et al. (2000) report a 50% mixture of trigonal plates and columns (based on Heymsfield (1986) replicator data collected in 1973). Also, the size of CR-AVE particles extended to 120 μm,

while McFarquhar et al. (2000) found the largest particles to be 50 μm, in both the 1973 study and an investigation in 1993 using a Learjet. The apparent difference in particle size may be due to instrumentation limitations used in the earlier studies (Lawson et al. 2006). However, the difference in the shape of the particles is real and is not readily explained. One (untested) possibility is that the very high relative humidity (up to 200%) observed by the WB-57F during CR-AVE was not present in the 1973 case reported by Heymsfield (1986). Based on a numerical model, Jensen et al. (2006) show that 3 to 4 ppmv water vapor (i.e., about 200% RH_{ice} at -80°C) is necessary to grow ice particles with sizes up to 100 μm.

Acknowledgments: This work was funded under NASA Grant No. NNG04GE71G.

REFERENCES

Baumgardner, D., H. Jonsson, W. Dawson, D. O'Connor and R. Newton, 2001: The cloud, aerosol and precipitation spectrometer: a new instrument for cloud investigations. *Atmos. Res.*, **59-60**, 251-264.

Beyerle, G., H.-J. Schäfer, R. Neuber, O. Schrems, and I. S. McDermid, 1998: Dual wavelength lidar observation of tropical high altitude cirrus clouds during the ALBATROSS 1996 campaign, *Geophys. Res. Lett.*, **25**, 919–922.

Comstock, J. M., Ackerman, T. P., and Mace, G. G, 2002: Ground based remote sensing of tropical cirrus clouds at Nauru Island: Cloud statistics and radiative impacts, *J. Geophys. Res.,* **107**, doi:10.1029/2002JD002 203.

Gierens, K. M., U. Schumann, M. Helten, H. Smit, and A. Marenco, 1999: A distribution law for relative humidity in the upper troposphere and lower stratosphere derived from three years of MOZAIC measurements, *Ann. Geophysicae*, **17**, 1218–1226.

Goldfarb, L., Keckhut, P., Chanin, M.-L., and Hauchecorne, A.2001: Cirrus climatological results from lidar measurements at OHP (44_ N, 6_ E), *Geophys. Res. Lett.*, **28**, 1687–1690.

Jensen, E. J., Toon, O. B., Pfister, L., and Selkirk, H. B, 1996: Dehydration of the upper troposphere and lower stratosphere by subvisible cirrus clouds near the tropical tropopause near the tropical tropopause, *Geophys. Res.Lett.*, **23**, 825–828.

Jensen, E. J., O. B. Toon, S. A. Vay, J. Ovarlez, R. May, P. Bui, C. H. Twohy, B. Gandrud, R. F. Pueschel, and U. Schumann, 2001: Prevalence of ice-supersaturated regions in the upper troposphere: Implications for optically thin ice cloud formation, *J. Geophys. Res.*, **106**, 17,253–17,266.

Jensen, E. J., L. Pfister, R. P. Lawson, B. Baker, Q. Mo, D. Baumgardner, E. M. Weinstock, J. B., Smith, M. J. Alexander, and O. B. Toon, 2006: Formation of Large (50-100 μm) Ice crystals Near the Tropical Tropopause. This conference.

Kärcher, B. and S. Solomon,1999: On the composition and optical extinction of particles in the tropopause region, *J. Geophys. Res*., **104**, 27,441–27,459.

Korolev, A.V., J.W. Strapp and G.A. Isaac, 1998: Evaluation of the accuracy of PMS optical array probes. *J. Atmos. Oceanic Technol.*, **15**, 708-720.

Lawson, R.P., B.A. Baker, C.G. Schmitt and T.L. Jensen, 2001: An overview of microphysical properties of Arctic clouds observed in May and July during FIRE.ACE. *J. Geophys. Res.*, **106**, 14,989-15,014.

Lawson, R. P., D. O'Connor, P. Zmarzly, K. Weaver, B. A. Baker, Q. Mo, and H. Jonsson, 2006: The 2D-S (Stereo) Probe: Design and Preliminary Tests of a New Airborne, High Speed, High-Resolution Particle Imaging Probe. In Press: *J. Atmos. Oceanic Technol.*, (Available at http://www.specinc.com/publications.htm)

Lelieveld, J., A. Bregman, H. A. Scheeren, J. Ström, K. S. Carslaw, H. Fischer, P. C. Siegmund, and F. Arnold, 1999: Chlorine activation and ozone destruction in the northern lowermost stratosphere, *J. Geophys. Res.*, **104**, 8201–8213.

May, R. D., 1998: Open path, near-infrared tunable diode laser spectrometer for atmospheric measurements of H_2O. *J. Geophys. Res*., **103,** 19161-19172**.**

McFarquhar, G. M., A. J. Heymsfield, J. Spinhirne, and B. Hart, 2000: Thin and subvisual tropopause tropical cirrus: Observations and radiative impacts, *J. Atmos. Sci.*, **57**, 1841–1853.

Sassen, K, M. K. Griffin, and G. C. Dodd, 1989: Optical scattering and microphysical properties of subvisible cirrus clouds, and climatic implications. *J. Appl. Meteor.,* **28,** 91–98.

Sassen, K. and J. R. Campbell, 2001: A midlatitude cirrus cloud climatology from the facility for atmospheric remote sensing. Part I: Macrophysical and synoptic properties, *J. Atmos. Sci.*, **58**, 481–496.